Daniel's Super Cool and overly long title

Daniel Mortensen, Jacob Gunther

***Abstract*—TODO: add abstract**

***Index Terms*—TODO: Add Keywords**

I. Introduction

Recent calls for a reduced carbon footprint have pushed transit authorities to adopt electric buses (EB). Conversion to EB reduces environmental impact as EB provide zero emissions and access to renewable energy [14].

These benefits are possible because EB draw power from electrical infrastructure. The loads introduced by charging are substantial and can exceed the grid capacity [16][6][3], requiring prohibitively expensive upgrades. The cost of upgrading is reflected in the billing structure used by power providers and can make large-scale charging undesireable for consumers.

One approach to reducing charge costs, is to defer premature upagrades by efficiently managing how buses charge. However, developing charge plans must consider a number of factors. All buses must maintain a minimum charge level while adhering to route schedules. When charging, batteries must have sufficient charge time and share a limited number of chargers. The focus of this work is to find an optimal charge schedule which meets these requirements while minimizing fiscal expenses from grid use. This problem is refered to hereafter as the 'charge problem'.

The remainder of this paper is organized as follows: Section II gives a description of previous work for solving the charge problem and Section III describes a graph-based framework for modeling the operations environment. Section IV extends the content of III to account for differences between day and night operations, and Section V incorporates the problem constraints involving battery charge dynamics. Sections VI and VII translate the rate schedule used for billing and into an objective function to minimize. Finally, Sections VIII, IX, and X briefly describe the optimization software used to solve the resulting mixed integer linear program developed in previous sections, presents results, and describes future work.

II. Literature Review

We acknowledge the existance of additional contributions, such as minimizing costs for startup infrastructure [17], and preserving battery lifespan [9]. However, as these are not relevent to this work, we consider them outside the scope of this review. We further acknowledge that some works cited herein contain solutions to several of these problems, such as in [20], but for sake of organization, we list them in the most relevent context.

A. Battery Charging

Here we consider solutions to empty batteries and focus our attention on either battery replacement or charging methods. We also refer to charging methods as either static (at rest) or dynamic (in motion).

Because charge times can significantly complicate logistics, [19] and [11] give methods for exchanging spent with charged batteries. The benefits include minimal down time as refueling can occur in a matter of minutes. Unfortunately, batteries can be cumbersome, and their exchange can be difficult. It also requires specialized tools, and could require automation.

Another alternative is to inductively charge buses while they traverse their routes [2], [11], [12], [5]. Unfortunately, this requires significant infrastructure which may not be available and is cost prohibitive for large systems.

Alternative solutions tend towards optimal planning. This allows for buses to charge in the traditional sense, minimizes additional infrastructure, and avoids the complexities of exchanging batteries. These approaches generally fall into one of three categories; reactive, hybrid, and global.

Reactive planning focuses strictly on presential circumstances. Methods of this type are computationally efficient, run in real-time, and are adaptable. These techniques generally stem from control theory and minipulate a current state to minimize cost. One such example includes the work done by [4], who uses comparable methodology to reduce demand on the power grid. This methodology however, does not account for global phenomena that require broader planning schemes and for the most part this class of technqiues remain unused for bus charging.

Another class of algorithms encompasses a limited number of projected events to improve decision making. This allows for a middle ground between simplicity and global planning and has proven useful in previous work [10], [1].

Global planning algorithms assume comlplete foreknowledge of future events and provide globally optimal plans [18],[7]. This class of algorithm requires more computation and is less flexible then reactive or hybrid approaches. However, the solutios are globally optimal and derive from insight unavailable to other algorithm classes.

B. Cost Management

The final set of constraints aim to decrease load on the grid. Previous work has shown that the use of electric buses can significantly complicate local power management [3] [6]. Additinally, power demand generally increases the fiscal cost from a billing perspective. [8] has provided methodology for forcasing the load on the grid. These types of models often form the basis for power distribution algorithms. For example, [15] gives an approach to minimize grid demand, but requires

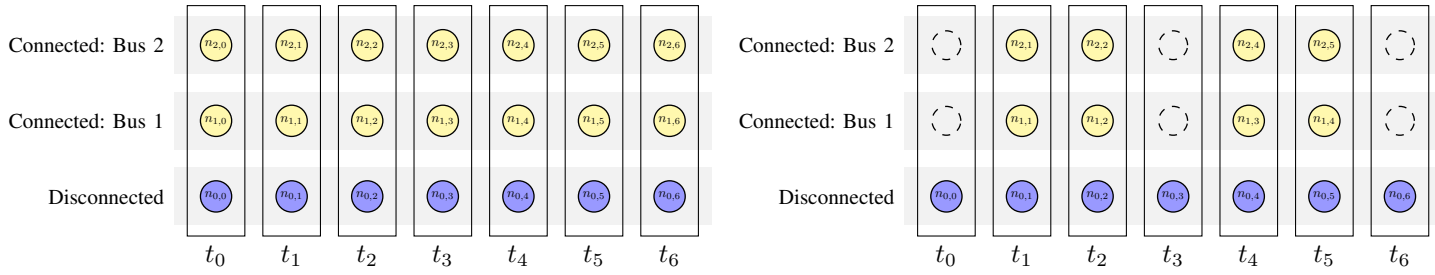

(a) Graph showing buses and timesteps

(b) two-bus scenario from figure 1a where each bus is absent at t_0, t_3, and t_6

Fig. 1: Bus availability represented in a graph

foreknowledge of uncontrolled loads. [4] takes a different approach and observes real-time data to control the charge rates of connected buses. [13] also operates in the real-time sense but uses on-board batteries to mitigate the effects of rapid charging.

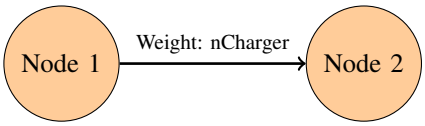

Fig. 2: Node to Node Connection

III. Graph Based Problem Formulation

A solution to the bus charge problem must reveal both *when* and *to which* bus a charger should connect. This suggests an approach with two dimensions, the first characterizing time and the second encoding charger connections as charge-states. This 2-D representation is encoded as a grid where time is given discretely in a left to right fashion and charge-states extend vertically as seen in figure 1a. In an effort to accurately represent charger use, the available charge-states include 'connected' states for each bus and a 'disconnected' state for idle periods. The intersection of charge-states and time indices is represented by a node, denoted $n_{i,j}$ which represents charge-state i at time t_j (see figure 1a).

A complete grid, however, implies that chargers can always connect to all buses. This is not always the case as a bus's schedule is divided into 'on-route' and 'in-station' segments. While on-route, buses depart to provide transit services and are unable to charge. To reflect this constraint, nodes are also used to denote availability and are removed when a bus is on-route (see figure 1b).

Transitions from one node to the next are called edges (see figure 2) and represent decisions to either connect, charge, not charge, or disconnect. The decision an edge represents is determined by the nodes to either side. An edge which exits and enters no-charge nodes represents a period where chargers are disconnected, resulting in a no-charge decision. Similarly, edges which both enter and exit charge nodes indicate a to-charge decision. Both to-charge and no-charge decisions transitions represent *horizontal* shifts in the graph and do not change the effective state of the charger. Conversely, transitions between no-charge and to-charge nodes represent effective state changes. A no-charge to charge connection is disconnected at t_j and connected at t_{j+1}, indicating a decision to connect. The same logic applies for a disconnection where an edge begins connected and ends disconnected (see figure 4). Hence, the bus charge problem can be described in terms of nodes and edges where nodes represent in-station time periods

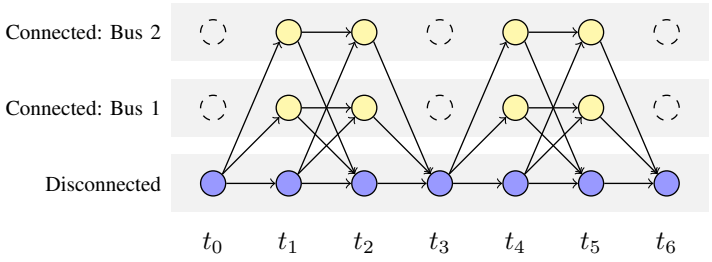

Fig. 3: Complete Problem formulation

and edges give all possible charge options as shown in figure 3.

Making decisions is encoded in the weight of each edge. The value of each weight is used to represent the number of chargers in the transition. For example, if two chargers were left unused from t_n to t_{n+1}, the corresponding edge would span two no-charge nodes, and have a weight value of two.

Consider a two-charger scenario where buses follow the schedule given in figure 3. A solution where Bus 1 charges

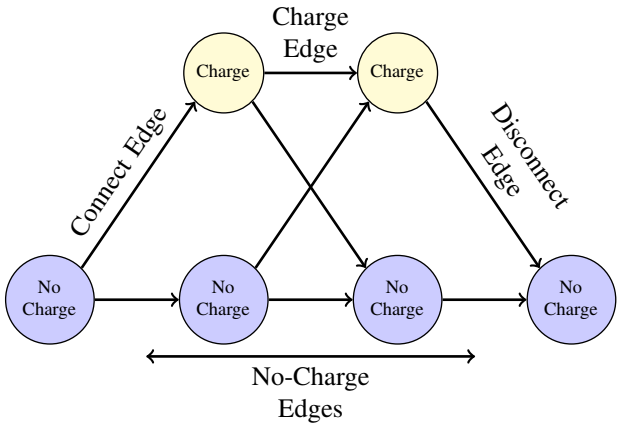

Fig. 4: Connect, Disconnect, and Charge Edges

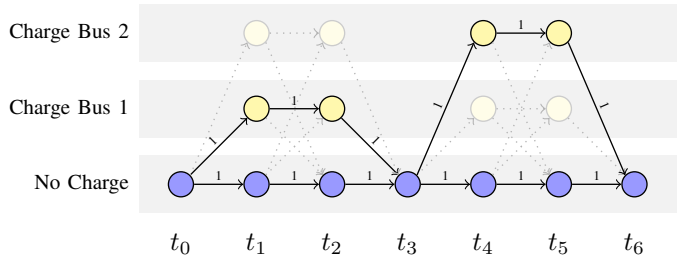

Fig. 5: One solution to a 2-bus 2-charger scenario

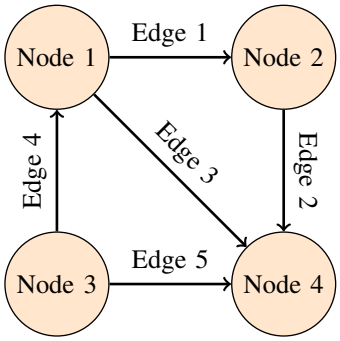

Fig. 6: A generic directed graph consisting of nodes and edges

from t_1 to t_2 and Bus 2 charges from t_4 to t_5 would be expressed by assigning non-zero weights to the appropriate connect, charge, and disconnect edges as shown in figure 5. Thus, solving the bus charge problem becomes a matter of finding the optimal set of edge weights.

To find the optimal set of weights, the graph must first be encoded in an incidence matrix. An incidence matrix organizes relationships between nodes and edges by describing which edges depart from and connect to which nodes. An incidence matrix A is an nNode $\times$ nEdge matrix where nNode is the number of nodes, and nEdge is the number of edges.

The columns of A describe connections for each edge and the rows give connections for each node. Incoming connections are represented with 1, outgoing connections with -1, and no connection with 0. For example, the graph in figure 6 is represented as:

$$\begin{bmatrix} -1 & 0 & -1 & 1 & 0 \\ 1 & -1 & 0 & 0 & 0 \\ 0 & 0 & 0 & -1 & -1 \\ 0 & 1 & 1 & 0 & 1 \end{bmatrix} \tag{1}$$

An incidence matrix can be used to find the number of chargers entering and leaving each state. None of the states (charging/non-charging) can create or destroy chargers and so the number of incoming must always equal the number of outgoing chargers. The only exception occurs at *source* and *sink* nodes.

A source node represents the beginning state of all chargers. Because a source state is the first, there are no incoming edges and hence, the net difference between incoming and outgoing chargers, or *the net-flow*, will be minus the number of chargers.

Sink nodes represent the final state, where all chargers enter and finish (see figure 7). Because sinks have no outgoing

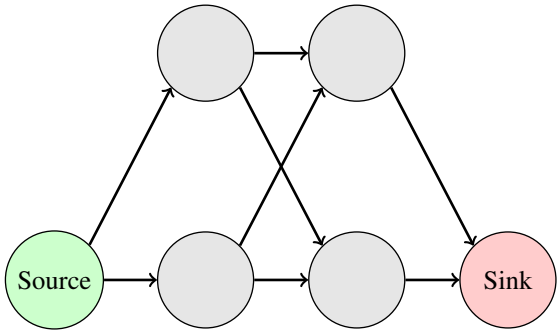

Fig. 7: Network flow illustrating sources and sinks

edges, they maintain a positive net-flow equal to the number of chargers.

Let x be a vector representing the edge weights, A be an adjacency matrix, and c_f be a vector where c_{f_i} gives the net-flow for the i^{th} node. The net-flow for each node can be expressed as

$$Ax = c_f \tag{2}$$

This expression can be used to constrain the net-flow of each node. c_f must equal zero for all non-source and non-sink elements and source/sink nodes must have net-flows equal to $-$nChargers and nChargers respectively (see equation 3).

$$Ax = \begin{bmatrix} 0 \\ \vdots \\ -\text{nCharger} \\ \vdots \\ 0 \\ \text{nCharger} \\ \vdots \\ 0 \end{bmatrix} \tag{3}$$

Flow can also be used to ensure that buses connect to only one charger at a time. Let a charge session, or *group*, be the set of all charge nodes between routes as shown in figure 8. The *group flow* is the number of chargers that enter a group and is represented as the sum of all incoming edge weights (see figure 9).

Let B be a nGroup $\times$ nEdge matrix where $B_{i,j}$ is 1 if the j^{th} edge enters the i^{th} group and 0 otherwise. For example, the B matrix corresponding to the graph in figure 10 contains 1 in the 7^{th} and 10^{th} columns for Group 1, and the 12^{th} and 15^{th} columns for group 2 as given in equation 4.

$$B = \begin{bmatrix} 0\,0\,0\,0\,0\,0\,1\,0\,0\,1\,0\,0\,0\,0\,0\,0 \\ 0\,0\,0\,0\,0\,0\,0\,0\,0\,0\,0\,1\,0\,0\,1\,0 \end{bmatrix} \tag{4}$$

Let x be the edge weights as before and c_g be an nGroup $\times$ 1 vector where the i^{th} element gives the group flow for group i. The group flow is then computed as

$$Bx = c_g \tag{5}$$

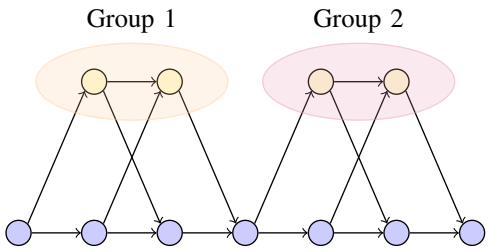

Fig. 8: Example of groups in a network flow graph

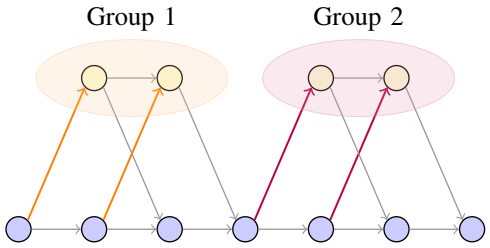

Fig. 9: Incoming Group Edges

But the group flow is required to be one at most. This is expressed by the inequality given in equation 6.

$$Bx \leq \begin{bmatrix} 1 \\ 1 \\ \vdots \\ 1 \end{bmatrix}, \tag{6}$$

IV. Battery State of Charge

Battery state of charge (SOC) also plays a large role in the bus charge problem. As a bus traverses a route, energy is discharged from the battery. If the battery state of charge drops to zero, the bus will power down and become unresponsive. It is therefore important to track battery charge levels when scheduling charge times.

Furthermore, as no charge actions are available while on route, SOC values are only tracked when in the charge station. Because these in-station time periods are also represented by the charge nodes from figure 1b, the two are in one-one correspondence. Consequently, every charge node$_{i,k}$ can be associated with an SOC value, denoted $d_{i,k}$ as shown in figure 11.

Charge level progression between $d_{i,k}$ and $d_{i,k+1}$ is influenced by two factors: discharging on route, and charging. The

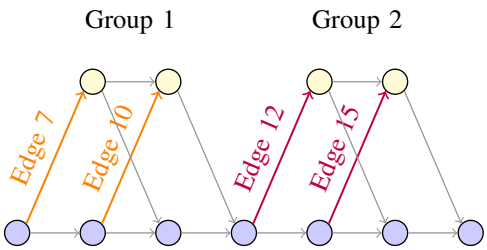

Fig. 10: Connect edge example for groups

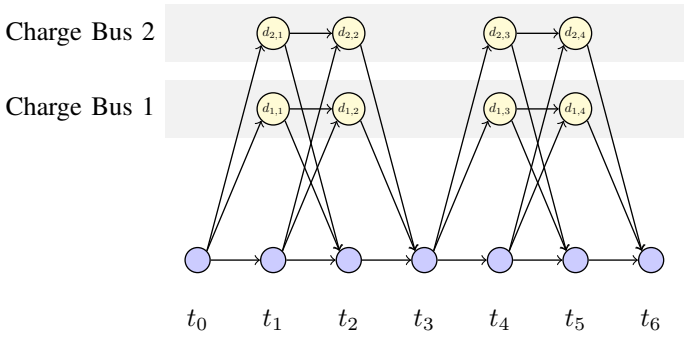

Fig. 11: SOC indicators

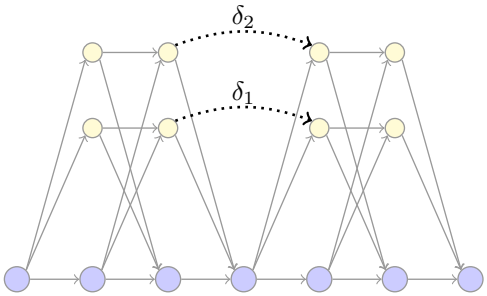

Fig. 12: δ values for routes

route discharge, denoted δ, represents the energy drawn from the battery in kWh. When a bus returns from a route, the change in SOC is computed as

$$d_{i,k+1} = d_{i,k} - \delta_i \tag{7}$$

where δ_i is the discharge for Bus i's route as seen in figure 12.

When a charger connects to a bus, the increase or *gain* in $d_{i,k}$ is denoted $g_{i,k}$, where i and k represent the respective bus and outgoing node indices. Figure 13 gives an example where $g_{1,1}$ and $g_{1,3}$ correspond to Bus 1's gain from t_0 to t_1 and t_4 to t_5.

Using a single charge rate however has drawbacks. If the rate is high, buses will charge quickly but the load on the grid will increase. Decreased charge rates will stress the grid less but increase charge time. To address both situations, a method

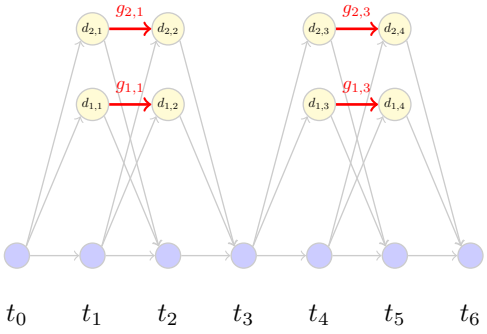

Fig. 13: Depiction of which edges increase SOC for the single rate case

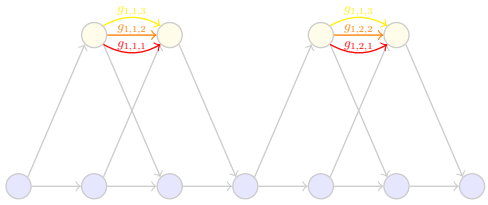

Fig. 14: Multi-Rate Charging

with additional flexibility must be used where both high and low charge rates are available.

Let $g_{i,k,l}$ be the gain, where i and k represent the bus and outgoing node indicies as before and l represents the charge rate index. Each charge rate index corresponds to an edge in the graph. Figure 14 gives an example where there are three rate options. Each rate corresponds to an edge between two charge nodes and together, all three edges provide multiple options for charging. These gains are used to compute succeeding charge levels as

$$d_{i,k+1} = d_{i,k} + \sum_{l} g_{i,k,l}, \tag{8}$$

but because of group and flow constraints, only one charge rate can be active at a time. Therefore, $d_{i,k}$ can be expressed as

$$d_{i,k+1} = d_{i,k} + g_{i,k,l}, \tag{9}$$

where the l^{th} charge edge is active.

$g_{i,k,l}$ is computed using the Constant Current Constant Voltage (CCCV) model as derived in [18] which gives:

$$d_{i,k+1} = \bar{a}_l d_{i,k} - \bar{b}_l M \tag{10}$$

Where $\bar{a}_l \sim (0, 1]$, depends on the charge rate and is experimentally determined, M is the battery charge capacity in kWh, and $\bar{b}_l = \bar{a}_l - 1$. Equations 9 and 10 are used to show that

$$\begin{aligned} & d_{i,k+1} = \bar{a}_l d_{i,k} - \bar{b}_l M \\ \Rightarrow & d_{i,k+1} - d_{i,k} = \bar{a}_l d_{i,k} - \bar{b}_l M - d_{i,k} \\ \Rightarrow & g_{i,k,l} = \bar{a}_l d_{i,k} - \bar{b}_l M - d_{i,k} \\ \Rightarrow & g_{i,k,l} = (\bar{a}_l - 1) d_{i,k} - \bar{b}_l M \end{aligned} \tag{11}$$

The results from equation 11, however, only hold when a charger is connected to a bus, which is represented by a weight of 1 for the edge corresponding to $g_{i,k,l}$. When the weight equals 0, $g_{i,k,l}$ must also equal zero. These two situations can be described using a switching constraint known as the *big M* technique. This technique is used to describe $g_{i,k,l}$ with equation 11 when the transition weight is 1 and $g_{i,k,l} = 0$ when 0.

$$\begin{aligned} & \begin{cases} g_{i,k,l} = d_{i,k}(\bar{a}_l - 1) - \bar{b}_l M & x_{i,k,l} = 1 \\ g_{i,k,l} = 0 & x_{i,k,l} = 0 \end{cases} \\ \Rightarrow & \begin{cases} g_{i,k,l} \le d_{i,k}(\bar{a}_l - 1) - \bar{b}_l M \\ g_{i,k,l} \ge d_{i,k}(\bar{a}_l - 1) - \bar{b}_l M & x_{i,k,l} = 1 \\ g_{i,k,l} \le 0 \\ g_{i,k,l} \ge 0 & x_{i,k,l} = 0 \end{cases} \end{aligned} \tag{12}$$

where $x_{i,k,l}$ is the edge weight corresponding to $g_{i,k,l}$. The piecewise function in equation 12 can be rewritten as

$$\begin{aligned} & \begin{cases} g_{i,k,l} \le d_{i,k}(\bar{a}_l - 1) - \bar{b}_l M \\ g_{i,k,l} \ge d_{i,k}(\bar{a}_l - 1) - \bar{b}_l M & x_{i,k,l} = 1 \\ g_{i,k,l} \le 0 \\ g_{i,k,l} \ge 0 & x_{i,k,l} = 0 \end{cases} \\ & g_{i,k,l} \le d_{i,k}(\bar{a}_l - 1) - \bar{b} M - M(1 - x_{i,k,l}) \\ \Rightarrow & g_{i,k,l} \ge d_{i,k}(\bar{a}_l - 1) - \bar{b} M \\ & g_{i,k,l} \le 0 + M x_{i,k,l} \\ & g_{i,k,l} \ge 0 \end{aligned} \tag{13}$$

The results of equation 13 obtain a switching effect. When $x_{i,k,l} = 1$, equation 13 becomes

$$\begin{aligned} g_{i,k,l} &\le d_{i,k}(\bar{a}_l - 1) - \bar{b}_l M \\ g_{i,k,l} &\ge d_{i,k}(\bar{a}_l - 1) - \bar{b}_l M \\ g_{i,k,l} &\le M \\ g_{i,k,l} &\ge 0. \end{aligned} \tag{14}$$

The active constraints imply equality for $g_{i,k,l} = (\bar{a}_l - 1) d_{i,k} - \bar{b}_l M$. The inactive constraints imply that $g_{i,k,l}$ is greater then zero, and less then the battery capacity. These constraints are also true, but have no effect on $g_{i,k,l}$. When $x_{i,k,l} = 0$, equation 13 becomes

$$\begin{aligned} g_{i,k,l} &\le d_{i,k}(\bar{a}_l - 1) - \bar{b}_l M - M \\ g_{i,k,l} &\ge d_{i,k}(\bar{a}_l - 1) - \bar{b}_l M \\ g_{i,k,l} &\le 0 \\ g_{i,k,l} &\ge 0. \end{aligned} \tag{15}$$

Where the inactive constraints indicate that $g_{i,k,l}$ is less then some positive value, and greater than a negative value. These constarints have no effect as the active constraints imply equality for $g_{i,k,l} = 0$.

Equation 13 can be expressed in linear form as

$$\begin{aligned} -g_{i,k,l} + d_{i,k}(\bar{a}_l - 1) + x_{i,k,l} &\le M(\bar{b}_l + 1) \\ g_{i,k,l} - d_{i,k}(\bar{a}_l - 1) &\le -\bar{b}_l M \\ g_{i,k,l} - M x_{i,k} &\le 0 \\ -g_{i,k,l} &\le 0. \end{aligned} \tag{16}$$

V. Multi-Graph Additions

An additional contribution this work offers is the expansion to night vs day charging. During the night, there is one charger for each bus; each with a single charge rate. During this time, buses are also available to charge at any time. These differences in operations introduce changes to the original graph formation and warrent a separate graph.

Night graphs consider a situation where both the number of buses reflecte the number of chargers and buses are readily available. Note how there are several source and sink nodes in figure 15. When a bus deploys for the day, the available number of charges changes and are reflected in the underlying source and sink constraints.

Changes in the first graph are reflected in the second through use of state of charge variables.

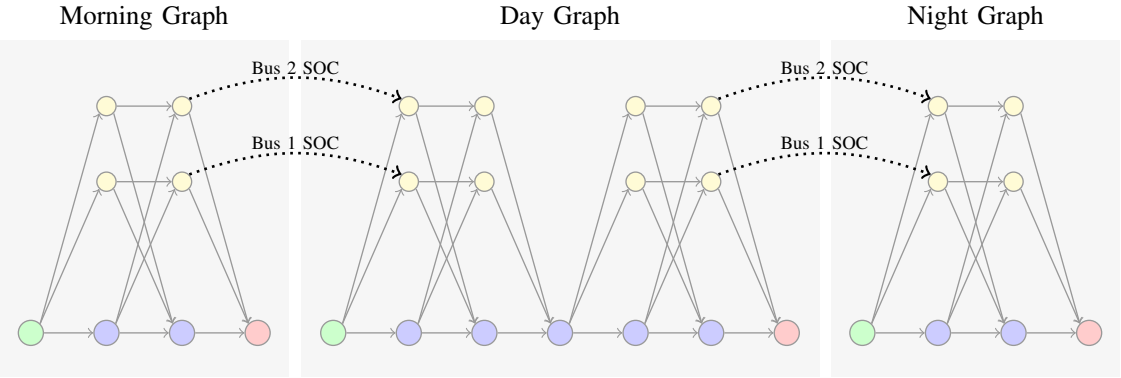

Fig. 15: Night vs Day Graphs

VI. Fiscal Rate Schedule

One objective of this work is to minimize the fiscal cost associated with power use and uses the Rocky Mountain Power schedule 8 billing rates. This billing schedule includes an on-peak power charge, facilities charge, and both on and off peak energy charges.

The facilities charge is computed by calculating the average power over a 15 minute period. The facilities charge is based on the maximum average value over the course of the month. This section of the bill charges $4.81 per kW. The On-Peak Power Charge is similarly calculated but only includes average values from designated on-peak hours. Rocky Mountain Power charges $15.73 per kW for this value.

the facilities power can be formulated as a linear set of constraints that include power used at each timestep for charging buses and external loads. This can be expressed as

$$c_i = \sum_j g_{i,j} + p_i$$

Where c_i represnets the

The energy charges are billed per kWh and charge for each unit of energy used. There are two rates: 5.8282¢for energy consumed during on-peak hours, and 2.6316¢for off-peak hours. general introduction with details for demand and consumption charge and how these relate to the end-of-the-month billing.

a. external loads (contribution) b. consumption charge i. total energy in Kwh ii. on-peak vs off-peak iii. constraints for consumption charge c. demand charge i. average power in 15 minute window ii. on-peak vs facilities iii. constraints for on-peak and facilities charges d. total cost breakdown i. Show how Rocky Mountain Power uses these and what the cost weighting is.

VII. Bus Fleet Operations

Overview of bus operations during the day vs the night a. night environment i. one charger per bus ii. slow chargers iii. single rate chargers iv. buses always available b. day environment i. limited number of chargers ii. fast/variable rates iii. limited charging availability c. multiple graphs to incorporate day vs night charging i. show picture to illustrate this ii. show SOC constraints to implement these relationships

VIII. Objective Function

IX. Gurobi & Usage

X. Results

XI. Future Work

REFERENCES

[1] Avishan Bagherinezhad et al. "Spatio-Temporal Electric Bus Charging Optimization With Transit Network Constraints". In: *IEEE Transactions on Industry Applications* 56.5 (Sept. 2020), pp. 5741–5749. ISSN: 0093-9994, 1939-9367. DOI: 10.1109/TIA.2020.2979132. URL: https://ieeexplore.ieee.org/document/9028116/ (visited on 11/13/2021).

[2] Bhagyashree J Balde and Arghya Sardar. "Electric Road system With Dynamic Wireless charging of Electric buses". In: *2019 IEEE Transportation Electrification Conference (ITEC-India)*. 2019 IEEE Transportation Electrification Conference (ITEC-India). Bengaluru, India: IEEE, Dec. 2019, pp. 1–4. ISBN: 978-1-72813-169-6. DOI: 10.1109/ITEC-India48457.2019.ITECINDIA2019-251. URL: https://ieeexplore.ieee.org/document/9080859/ (visited on 11/18/2021).

[3] T. Boonraksa et al. "Impact of Electric Bus Charging on the Power Distribution System a Case Study IEEE 33 Bus Test System". In: *2019 IEEE PES GTD Grand International Conference and Exposition Asia (GTD Asia)*. 2019 IEEE PES GTD Grand International Conference and Exposition Asia (GTD Asia). Bangkok, Thailand: IEEE, Mar. 2019, pp. 819–823. ISBN: 978-1-5386-7434-5. DOI: 10.1109/GTDAsia.2019.8716023. URL: https://ieeexplore.ieee.org/document/8716023/ (visited on 11/13/2021).

[4] Qifu Cheng et al. "A smart charging algorithm-based fast charging station with energy storage system-free". In: *CSEE Journal of Power and Energy Systems* (2020). ISSN: 20960042, 20960042. DOI: 10.17775/CSEEJPES.2020.00350. URL: https://ieeexplore.ieee.org/stamp/stamp.jsp?tp=&arnumber=9171658 (visited on 11/19/2021).

[5] Blint Csonka. "Optimization of Static and Dynamic Charging Infrastructure for Electric Buses". In: *Energies* 14.12 (June 13, 2021), p. 3516. ISSN: 1996-1073. DOI: 10.3390/en14123516. URL: https://www.mdpi.com/1996-1073/14/12/3516 (visited on 11/13/2021).

[6] Sanchari Deb, Karuna Kalita, and Pinakeshwar Mahanta. "Impact of electric vehicle charging stations on reliability of distribution network". In: *2017 International Conference on Technological Advancements in Power and Energy (TAP Energy)*. 2017 International Conference on Technological Advancements in Power and Energy (TAP Energy). Kollam: IEEE, Dec. 2017, pp. 1–6. ISBN: 978-1-5386-4021-0. DOI: 10.1109/TAPENERGY.2017.8397272. URL: https://ieeexplore.ieee.org/document/8397272/ (visited on 11/16/2021).

[7] Nader A. El-Taweel and Hany E. Z. Farag. "Incorporation of Battery Electric Buses in the Operation of Intercity Bus Services". In: *2019 IEEE Transportation Electrification Conference and Expo (ITEC)*. 2019 IEEE Transportation Electrification Conference and Expo (ITEC). Detroit, MI, USA: IEEE, June 2019, pp. 1–6. ISBN: 978-1-5386-9310-0. DOI: 10.1109/ITEC.2019.8790598. URL: https://ieeexplore.ieee.org/document/8790598/ (visited on 11/19/2021).

[8] Qiang Gao et al. "Charging Load Forecasting of Electric Vehicle Based on Monte Carlo and Deep Learning". In: *2019 IEEE Sustainable Power and Energy Conference (iSPEC)*. 2019 IEEE Sustainable Power and Energy Conference (iSPEC). Beijing, China: IEEE, Nov. 2019, pp. 1309–1314. ISBN: 978-1-72814-930-1. DOI: 10.1109/iSPEC48194.2019.8975364. URL: https://ieeexplore.ieee.org/document/8975364/ (visited on 11/19/2021).

[9] Adnane Houbbadi et al. "Optimal Charging Strategy to Minimize Electricity Cost and Prolong Battery Life of Electric Bus Fleet". In: *2019 IEEE Vehicle Power and Propulsion Conference (VPPC)*. 2019 IEEE Vehicle Power and Propulsion Conference (VPPC). Hanoi, Vietnam: IEEE, Oct. 2019, pp. 1–6. ISBN: 978-1-72811-249-7. DOI: 10.1109/VPPC46532.2019.8952493. URL: https://ieeexplore.ieee.org/document/8952493/ (visited on 11/13/2021).

[10] Amra Jahic, Mina Eskander, and Detlef Schulz. "Preemptive vs. non-preemptive charging schedule for large-scale electric bus depots". In: *2019 IEEE PES Innovative Smart Grid Technologies Europe (ISGT-Europe)*. 2019 IEEE PES Innovative Smart Grid Technologies Europe (ISGT-Europe). Bucharest, Romania: IEEE, Sept. 2019, pp. 1–5. ISBN: 978-1-5386-8218-0. DOI: 10.1109/ISGTEurope.2019.8905633. URL: https://ieeexplore.ieee.org/document/8905633/ (visited on 11/16/2021).

[11] Shubham Jain et al. "Battery Swapping Technology". In: *2020 5th IEEE International Conference on Recent Advances and Innovations in Engineering (ICRAIE)*. 2020 5th IEEE International Conference on Recent Advances and Innovations in Engineering (ICRAIE). Jaipur, India: IEEE, Dec. 1, 2020, pp. 1–4. ISBN: 978-1-72818-867-6. DOI: 10.1109/ICRAIE51050.2020.9358366. URL: https://ieeexplore.ieee.org/document/9358366/ (visited on 11/18/2021).

[12] Seog Y. Jeong et al. "Automatic Current Control by Self-Inductance Variation for Dynamic Wireless EV Charging". In: *2018 IEEE PELS Workshop on Emerging Technologies: Wireless Power Transfer (Wow)*. 2018 IEEE PELS Workshop on Emerging Technologies: Wireless Power Transfer (WoW). Montral, QC, Canada: IEEE, June 2018, pp. 1–5. ISBN: 978-1-5386-2465-4. DOI: 10.1109/WoW.2018.8450926. URL: https://ieeexplore.ieee.org/document/8450926/ (visited on 11/18/2021).

[13] Inaki Ojer et al. "Development of energy management strategies for the sizing of a fast charging station for electric buses". In: *2020 IEEE International Conference on Environment and Electrical Engineering and 2020 IEEE Industrial and Commercial Power Systems Europe (EEEIC / I&CPS Europe)*. 2020 IEEE International Conference on Environment and Electrical Engineering and 2020 IEEE Industrial and Commercial Power Systems Europe (EEEIC / I&CPS Europe). Madrid, Spain:

IEEE, June 2020, pp. 1–6. ISBN: 978-1-72817-455-6. DOI: 10.1109/EEEIC/ICPSEurope49358.2020.9160716. URL: https://ieeexplore.ieee.org/document/9160716/ (visited on 11/16/2021).

[14] Kavuri Poornesh, Kuzhivila Pannickottu Nivya, and K. Sireesha. "A Comparative study on Electric Vehicle and Internal Combustion Engine Vehicles". In: *2020 International Conference on Smart Electronics and Communication (ICOSEC)*. 2020 International Conference on Smart Electronics and Communication (ICOSEC). Trichy, India: IEEE, Sept. 2020, pp. 1179–1183. ISBN: 978-1-72815-461-9. DOI: 10.1109/ICOSEC49089.2020.9215386. URL: https://ieeexplore.ieee.org/document/9215386/ (visited on 11/13/2021).

[15] Nan Qin et al. "Numerical analysis of electric bus fast charging strategies for demand charge reduction". In: *Transportation Research Part A: Policy and Practice* 94 (Dec. 2016), pp. 386–396. ISSN: 09658564. DOI: 10.1016/j.tra.2016.09.014. URL: https://linkinghub.elsevier.com/retrieve/pii/S096585641630444X (visited on 11/13/2021).

[16] Daniel Stahleder et al. "Impact Assessment of High Power Electric Bus Charging on Urban Distribution Grids". In: *IECON 2019 - 45th Annual Conference of the IEEE Industrial Electronics Society*. IECON 2019 - 45th Annual Conference of the IEEE Industrial Electronics Society. Lisbon, Portugal: IEEE, Oct. 2019, pp. 4304–4309. ISBN: 978-1-72814-878-6. DOI: 10.1109/IECON.2019.8927526. URL: https://ieeexplore.ieee.org/document/8927526/ (visited on 11/16/2021).

[17] Ran Wei et al. "Optimizing the spatio-temporal deployment of battery electric bus system". In: *Journal of Transport Geography* 68 (Apr. 2018), pp. 160–168. ISSN: 09666923. DOI: 10.1016/j.jtrangeo.2018.03.013. URL: https://linkinghub.elsevier.com/retrieve/pii/S0966692317306294 (visited on 11/13/2021).

[18] Justin Whitaker et al. "A Network Flow Approach to Battery Electric Bus Scheduling". In: (2021), p. 10.

[19] Xian Zhang and Guibin Wang. "Optimal dispatch of electric vehicle batteries between battery swapping stations and charging stations". In: *2016 IEEE Power and Energy Society General Meeting (PESGM)*. 2016 IEEE Power and Energy Society General Meeting (PESGM). Boston, MA, USA: IEEE, July 2016, pp. 1–5. ISBN: 978-1-5090-4168-8. DOI: 10.1109/PESGM.2016.7741893. URL: http://ieeexplore.ieee.org/document/7741893/ (visited on 11/18/2021).

[20] Dan Zhou et al. "Optimization Method of Fast Charging Buses Charging Strategy for Complex Operating Environment". In: *2018 2nd IEEE Conference on Energy Internet and Energy System Integration (EI2)*. 2018 2nd IEEE Conference on Energy Internet and Energy System Integration (EI2). Beijing: IEEE, Oct. 2018, pp. 1–6. ISBN: 978-1-5386-8549-5. DOI: 10.1109/EI2.2018.8582378. URL: https://ieeexplore.ieee.org/document/8582378/ (visited on 11/13/2021).